JOURNAL OF STRUCTURAL BIOLOGY 115, 250–257 (1995)

Three-Dimensional Reconstruction of Thick Filaments from Rapidly Frozen, Freeze-Substituted Tarantula Muscle

RAÚL PADRÓN, LORENZO ALAMO, JOSE REINALDO GUERRERO, AND MARISTELA GRANADOS

Laboratorio de Biología Estructural, Instituto Venezolano de Investigaciones Cientificas (IVIC), Apdo 21827, Caracas 1020A, Venezuela

AND

PEDRO UMAN AND ROGER CRAIG

Department of Cell Biology, University of Massachusetts Medical School, 55 Lake Avenue North, Worcester, Massachusetts 01655

Received December 19, 1994, and in revised form July 20, 1995

We have applied three-dimensional helical reconstruction techniques to images of myosin filaments of tarantula leg muscle obtained from rapidly frozen, freeze-substituted specimens. Computed Fourier transforms of filaments selected from longitudinal sections show up to six layer lines indexing on the 43.5-nm helical repeat of myosin crossbridges. The three-dimensional reconstruction, performed after separation of overlapped Bessel functions, shows four continuous strands of density on the surface of the filament, modulated by density at 14.5-nm intervals, corresponding to the myosin heads aligned approximately along the helical strands. In transverse view, the reconstruction shows four projections and is similar in profile to myosin filaments seen in thin transverse sections of rapidly frozen muscle. The reconstruction is similar to that of negatively stained, isolated tarantula filaments except that in the latter there is an additional modulation of the helix density, which better resolves the two heads of each myosin crossbridge. Thus, the general arrangement of the myosin heads in the freeze-substituted specimens is preserved, although finer details of structure such as individual myosin heads are lost. © 1995 Academic Press, Inc.

INTRODUCTION

Myosin filaments in striated muscle are constructed from bipolar, helical arrays of myosin molecules which interact with actin filaments to generate muscle shortening (Huxley, 1963, 1969). The arrangement and conformation of the myosin heads (crossbridges) *in situ* have been studied by X-ray diffraction of intact muscle (Huxley and Brown, 1967; Wray *et al.*, 1975). The crossbridge arrangements have been found to have helical and rotational symmetries which vary depending on muscle and species, and axial repeats (14.3–14.5 nm) that are constant in all muscles (Squire, 1971; Wray *et al.*, 1975; Tregear, 1984). However, precise rotational symmetries and detailed crossbridge structure have not been determined by X-ray diffraction owing to the absence of phase information.

More detailed and unambiguous information has come from electron microscopy of negatively stained or frozen-hydrated, isolated filaments. Three-dimensional helical reconstructions reveal the rotational and helical symmetries of the filaments and the structure of the crossbridges (Stewart *et al.*, 1981, 1985; Vibert and Craig, 1983; Crowther *et al.*, 1985; Kensler and Stewart, 1983, 1986, 1989; Stewart and Kensler, 1986; Morris *et al.*, 1991; Vibert, 1992). In most cases in which the two heads of a crossbridge have been resolved, the myosin heads have their long axis oriented approximately along the long-pitch helices, with one head of each molecule pointing toward the tip of the filament and the other toward the bare zone (Crowther *et al.*, 1985; Stewart *et al.*, 1985).

The detailed *in situ* structure of myosin filaments has not been determined by conventional electron microscopy sectioning techniques because of the deleterious effects of standard chemical fixation, dehydration, and embedding on filament structure (cf. Reedy, 1976; Reedy *et al.*, 1983). Recent studies have used rapid freezing as a means of rapid physical fixation of molecular structure of striated muscle *in situ*. After rapid freezing, specimens are processed by freeze-fracture (Heuser and Cooke, 1983; Tsukita and Yano, 1986), by freeze-substitution (Tsukita and Yano, 1985, 1986, 1988; Nassar *et al.*, 1986; Padrón *et al.*, 1988, 1992; Hirose and Wakabayashi, 1988, 1991, 1993; Padrón and Craig, 1989; Edelman, 1989; Lepault *et al.*, 1991; Craig *et al.*, 1992; Hirose *et al.*, 1993; Sosa *et al.*, 1994), or by cryosectioning and

1047-8477/95 $12.00

cryo-observation (McDowall *et al.*, 1984). Rapid freezing followed by freeze-substitution has resulted in excellent preservation of myosin filament helical structure in the relaxed filament lattice (e.g., Padrón and Craig, 1989; Craig *et al.*, 1992; Padrón *et al.*, 1992), and the rotational symmetries can now be observed directly along with some fine details of crossbridge structure (Craig *et al.*, 1991; Padrón *et al.*, 1993).

In this paper we have carried out a three-dimensional helical reconstruction of myosin filaments observed in longitudinal sections of rapidly frozen, freeze-substituted tarantula striated muscle. This reconstruction has been compared with that computed from negatively stained, isolated filaments (Crowther *et al.*, 1985) and with the average image obtained from transverse sections of rapidly frozen tarantula muscle (Padrón *et al.*, 1993). These results have been presented in preliminary form (Padrón *et al.*, 1994).

MATERIALS AND METHODS

Electron micrographs of rapidly frozen, chemically skinned tarantula muscle, freeze-substituted in the presence of 0.2% tannic acid, were those obtained by Padrón *et al.* (1992).

Three-dimensional helical reconstructions were computed from myosin filaments in longitudinal sections. The filaments used in the reconstructions were selected to show a fairly symmetrical mirror plane (Fig. 1a), implying that they had been included symmetrically within the section thickness, which was about 40 nm—comparable to the filament diameter. Care was taken to avoid thicker regions so that filaments would not be superimposed on one another. Electron micrograph negatives were digitized on a raster corresponding to an 0.8-nm sampling of the original specimen (Padrón *et al.*, 1992). All images were oriented in the same way (bare zone always at the same end) before digitization. Three-dimensional helical reconstructions were performed using programs from the MRC Laboratory of Molecular Biology image processing package adapted to run on a UNIX workstation (Sun SPARCstation II). The helical repeat used in the reconstructions was 43.5 nm (derived from X-ray diffraction of tarantula muscle; Wray, 1982). The three-dimensional (3D) reconstruction procedure, including the separation of Bessel function contributions on different layer lines, was performed as described by Crowther *et al.* (1985). Independent reconstructions, initially made from two sets of filaments, one with four and the other with three particles, agreed well with each other. Both sets were then combined to make the reconstruction to be described here. The helix was assumed to be right-handed, based on unidirectional shadowing information (Crowther *et al.*, 1985). Bessel terms were separated up to $J_{\pm 12}$ for the rapidly frozen specimens following the procedure of Crowther *et al.* (1985), as shown in the data plotted in Fig. 3. An estimated diameter of 35 nm was used for this separation (average of the 36.6-nm diameter from the filament profile and the 33.4-nm diameter calculated from the position of the first subsidiary peak of the J_0 Bessel function measured on the third layer line of the transforms). For comparison with the rapidly frozen, sectioned filaments, a new 3D map was also made from negatively stained filaments using the original Bessel-separated data of Crowther *et al.* (1985). 3D maps were rendered on a SUN SPARCstation LX using AVS software (Advanced Visual Systems, Inc., Waltham, MA) and were recorded on a Solitaire 8 Image Recorder (Management Graphics, Minneapolis, MN).

RESULTS

Figure 1a shows the seven filament images from rapidly frozen, freeze-substituted tarantula muscle used in the reconstruction. Contrast-reversed images of the eight negatively stained, isolated filaments from Crowther *et al.* (1985) used in the com-

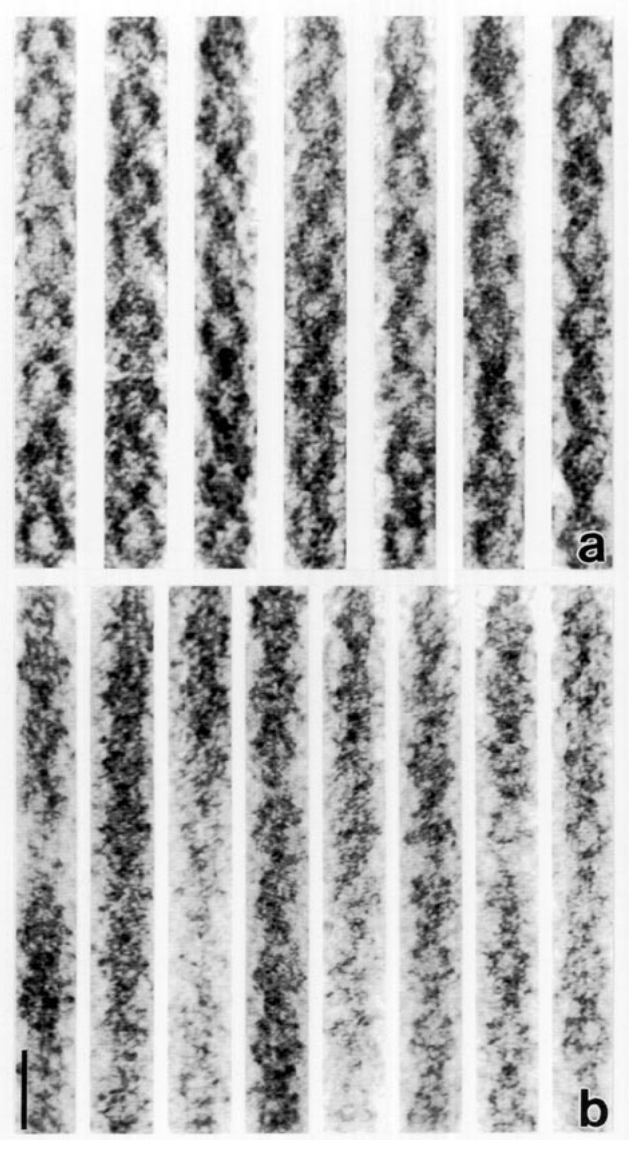

FIG. 1. Panel of the tarantula myosin filaments used in the three-dimensional helical reconstructions: (a) from longitudinal sections of freeze-substituted, skinned muscle and (b) from negatively stained homogenate of tarantula muscle, redigitized from Crowther *et al.* (1985). The diameter of the filaments, measured by plotting their average transverse profile, was 36.6 nm for the rapidly frozen specimens and 30.4 nm for the negatively stained specimens (cf. 32 nm quoted by Crowther *et al.*, 1985): this difference was probably due to sectioning artifacts or to the effect of the tannic acid used in the freeze-substitution. To facilitate comparison, the filaments in (b) have been scaled radially to have the same diameter as those in (a), and their contrast has been reversed. All the filaments are oriented such that the bare zone would appear at the top of the image. Scale bar, 50 nm.

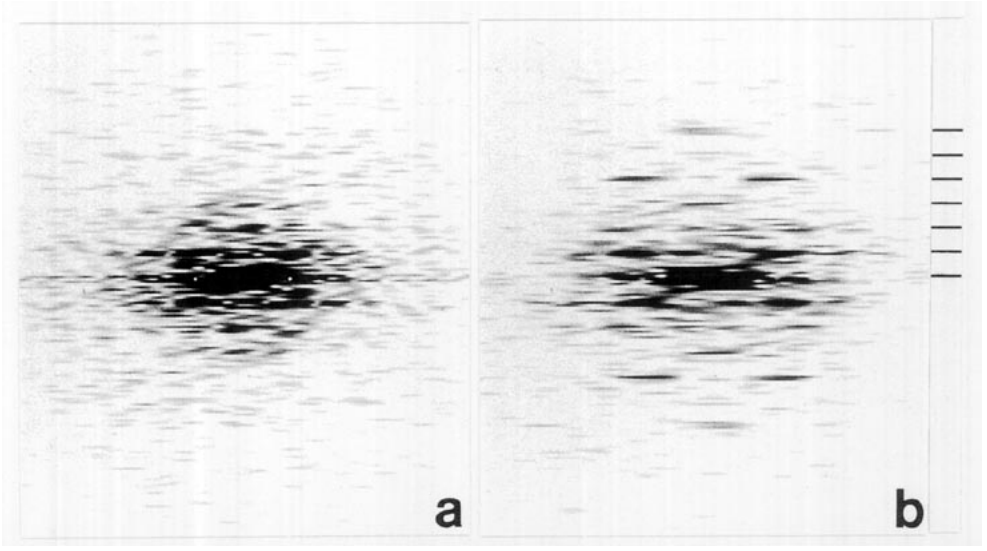

FIG. 2. Computed Fourier transforms of myosin filaments used in the 3D reconstructions: (a) from freeze-substituted, skinned muscle (corresponding to the sixth image in Fig. 1a) and (b) from negatively stained filaments (corresponding to the seventh image of Fig. 1b). Markers indicate orders of the 43.5-nm repeat.

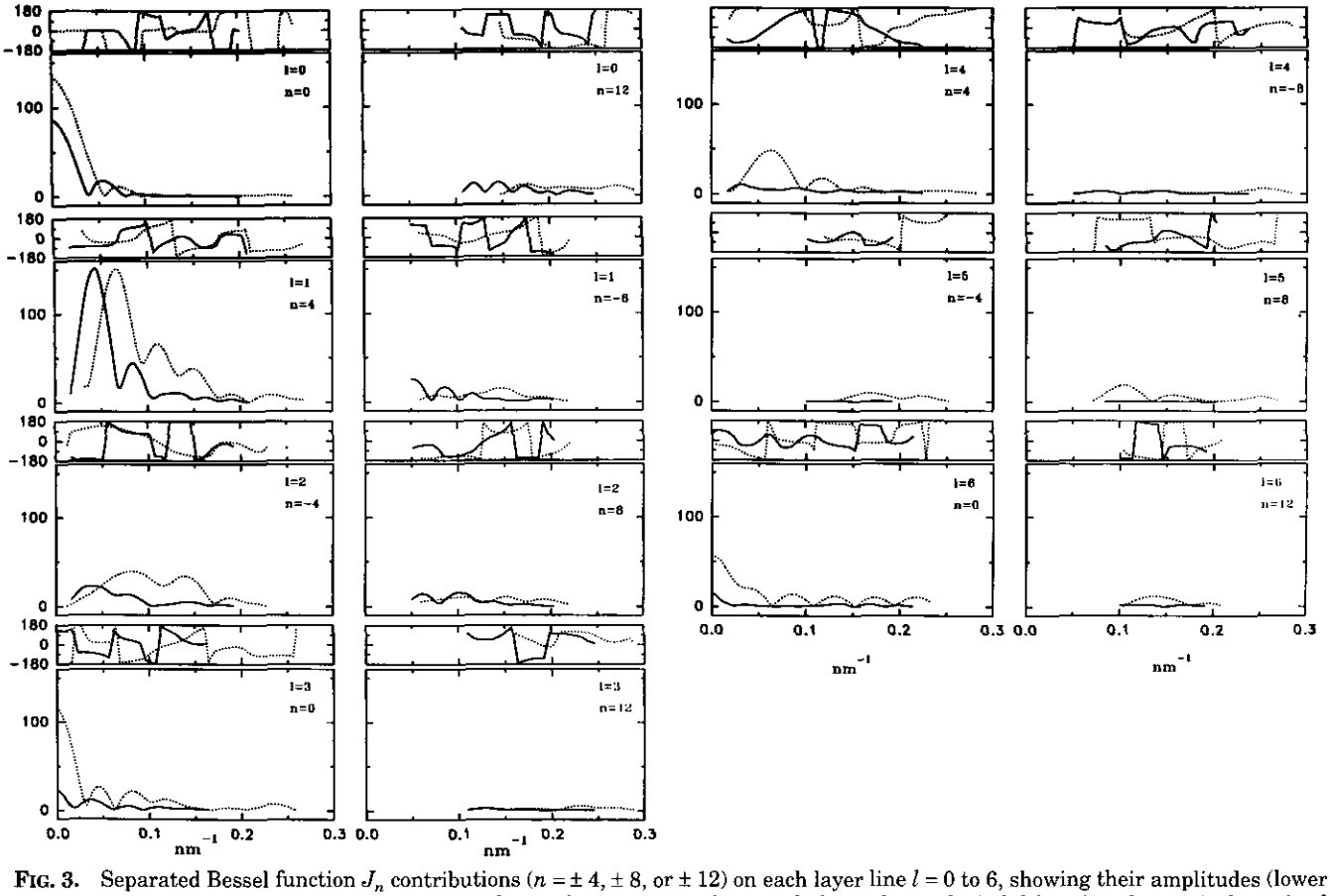

FIG. 3. Separated Bessel function J_n contributions ($n = \pm 4, \pm 8$, or ± 12) on each layer line $l = 0$ to 6, showing their amplitudes (lower part of each panel) and phases (upper part of each panel) for freeze-substituted skinned muscle (solid lines) and negatively stained filaments (dotted lines; from Crowther *et al.*, 1985). The amplitude of the $l = 0$, $n = 0$ term is plotted at one-tenth the scale of the others. The amplitudes for the freeze-substituted skinned muscle were scaled such that the peak of the $l = 1$, $n = 4$ term of the first layer line was made equal to the corresponding peak of the negatively stained filaments.

parison reconstruction are shown in Fig. 1b. Both sets of images show clear preservation of helical structure. The Fourier transforms (intensities) of the rapidly frozen filaments show up to six layer lines indexing on the 43.5-nm repeat (Fig. 2a), while those of the negatively stained filaments show intensity out to the ninth layer line (Fig. 2b). The radial extent of the two transforms is similar. When the transforms are compared, those from the rapidly frozen specimens are found to be weaker overall, the fourth and fifth layer lines in particular being much weaker than in the negatively stained filaments. In the transforms of the rapidly frozen specimens, the reflections from one side were generally stronger than those from the other side. This may have been due to preferential staining of one side of the specimens or to removal of part of the filament during the sectioning procedure. The latter is less likely because of the precautions taken in selecting filaments for reconstruction (see Materials and Methods).

Because of the even rotational symmetry of the tarantula myosin filaments ($N = 4$; Levine *et al.*, 1993; Crowther *et al.*, 1985; Padrón *et al.*, 1993), Bessel functions start to overlap at relatively low resolution (Crowther *et al.*, 1985). We have therefore computationally separated the Bessel contributions for each layer line $l = 0$–6 of the rapidly frozen specimens following the procedure of Crowther *et al.* (1985). The separated Bessel function contributions to these layer lines, $J_{\pm 4}$, $J_{\pm 8}$, and $J_{\pm 12}$, are shown in Fig. 3, and data on the fitting of the particles are summarized in Table I. For comparison, Bessel-separated data for the negatively stained filaments studied by Crowther *et al.* (1985) are also shown in Fig. 3 and their fitting data in Table I. The amplitudes for the rapidly frozen specimens are, in general, weaker than those for the negatively stained ones, and their peaks are shifted to a smaller radial spacing due to the larger filament diameter.

A three-dimensional reconstruction of the rapidly frozen, freeze-substituted specimens was calculated using the Bessel-separated data shown in Fig. 3. To evaluate the preservation attainable by the rapid freezing technique, this reconstruction was compared with that obtained using the Bessel-separated data from the negatively stained filaments. Data used in the reconstruction were included axially to 1/7.2 nm^{-1} (sixth layer line) for the rapidly frozen specimens and 1/4.8 nm^{-1} (ninth layer line) for the negatively stained ones. For both reconstructions, data were included to about 1/5 nm^{-1} radially. Figure 4 shows surface renderings of the three-dimensional reconstructions of the rapidly frozen (a and c) and negatively stained (b and d) specimens. Both maps show four helical tracks of density on the surface, with a helical repeat of 43.5 nm (see Materials and Methods), modulated at 14.5-nm levels, the axial distance between adjacent crossbridge levels. A difference between the reconstructions is the absence of finer details of structure in the map from the rapidly frozen specimens, corresponding to the weakness of the higher-order layer lines when compared with the negatively stained specimens. The rendering of the negative stain reconstruction (Fig. 4b) directly shows the features we interpreted before as the two heads of each myosin molecule pointing in opposite directions along the helical strands (Crowther *et al.*, 1985). The map from the rapidly frozen specimens (Fig. 4a) is roughly similar except that the two heads are not resolved from each other. Instead, each strand mimics roughly the envelope of the more detailed strand seen in Fig. 4b.

We have tested the validity of the reconstructions produced using rapid freezing and negative staining techniques by comparing them with independent observations, in which we do not rely on the assump-

TABLE I

Summary of Data on Fitting of Particles Used in Bessel Separation and 3D Reconstruction[a]

Particle number	View angle (degrees)[b]	Phase residual[c]	Least-squares residual[d]
	Rapidly frozen specimens		
855a	10.5	51	0.26
855b	0	28	0.29
858a	–7.5	64	0.24
861a	16.3	57	0.22
865b	16.8	48	0.23
869b	8.5	48	0.30
869d	9	58	0.33
	Negatively stained specimens[e]		
758-3	9	51	0.29
761-1	6.5	53	0.34
769-1	27.5	49	0.33
793-1	21	50	0.37
811-1	7	38	0.37
811-2	15	50	0.29
758-1	17	50	0.31
826-1	0	—	0.24

[a] Particles are listed in the order shown from left to right in Figs. 1a and 1b.

[b] Angular orientation of the particle relative to the average of the near and far sides of 855b or 826-1 as references.

[c] Weighted phase residual (see Crowther *et al.*, 1985) in degrees at the optimal position for fitting each particle against the averaged data from 855b or 826-1 as references. Data close to the meridian on layer line $l = 1$ to $l = 9$ are included.

[d] Least-squares residuals (see Crowther *et al.*, 1985) from the Bessel separation program, corresponding to the lack of fit in solving equation (1) in Crowther *et al.* (1985). All data from layer lines $l = 1$ to $l = 9$ included but $l = 0$ excluded as its strength would dominant the weighting.

[e] Data from Crowther *et al.* (1985) corresponding to the eight negatively stained specimens are shown for comparison purposes.

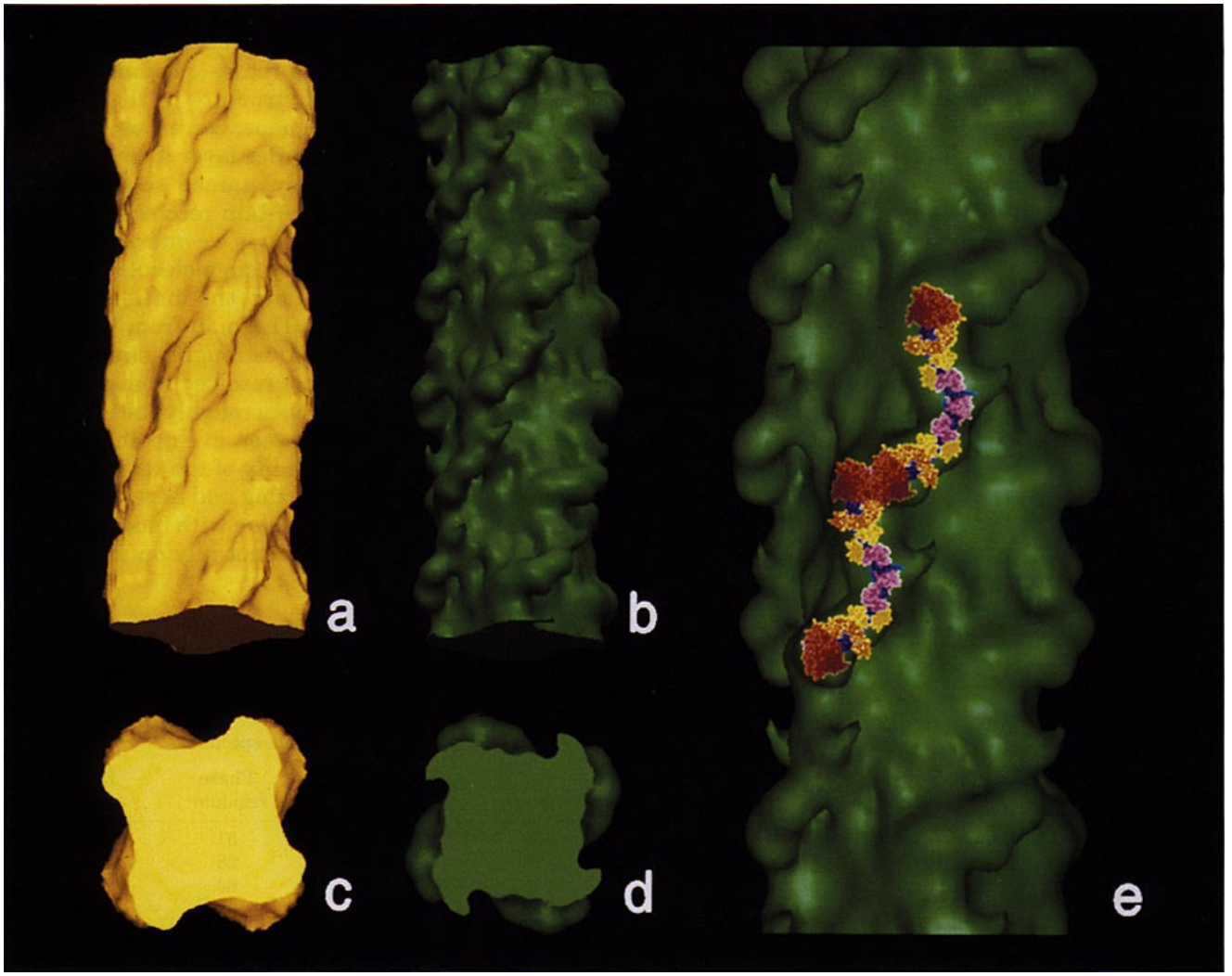

FIG. 4. Surface renderings of three-dimensional helical reconstructions of myosin filaments. (a and b) Longitudinal views of segments containing six 14.5-nm crossbridge repeats; (c and d) transverse views of 14.5-nm-long segments (one repeat, from 7.5 up to 22 nm from the bottom of the reconstructions shown in (a and b)). (a and c) From freeze-substituted, skinned muscle; (b and d) from negatively stained filaments. (b and d) Recalculated from the original Bessel-separated data of Crowther *et al.* (1985); (e) enlarged view of the central region of (b) with the space filling representation of S1 (modified from original image provided by Dr I. Rayment (Rayment *et al.*, 1993)) oriented approximately by eye on the envelope of one of the four helices of the 3D reconstruction.

tion of helical symmetry. Projections (Figs. 5a and 5b) of transverse views of one crossbridge level of the 3D density maps (Figs. 4c and 4d) are similar to averaged or rotationally filtered images obtained from transversely cut thin sections of rapidly frozen muscle (Figs. 5c and 5d). The transverse sections directly confirm the fourfold symmetry of the reconstructions (Padrón *et al.*, 1993). The shape of each protruding feature (crossbridge) is similar in the transverse sections (Figs. 5c and 5d) and in the transverse projections (Figs. 5a and 5b) of the maps.

DISCUSSION

Our goal in this paper was to compute a three-dimensional helical reconstruction of myosin filaments observed in the intact filament lattice of muscle. This has been made possible by the good preservation of the myosin crossbridge helices that is provided by the rapid freezing, freeze-substitution technique: preservation is especially good in the case of invertebrate muscles, such as tarantula, which have more stable crossbridge arrays than vertebrates.

The map computed from longitudinal sections shows four helically arranged strands of density protruding to an outermost radius of about 20 nm (cf. 16 nm in negatively stained specimens, Crowther *et al.*, 1985). The validity of this reconstruction is supported by comparing the rapidly frozen filaments, and their 3D reconstruction, with three-dimensional

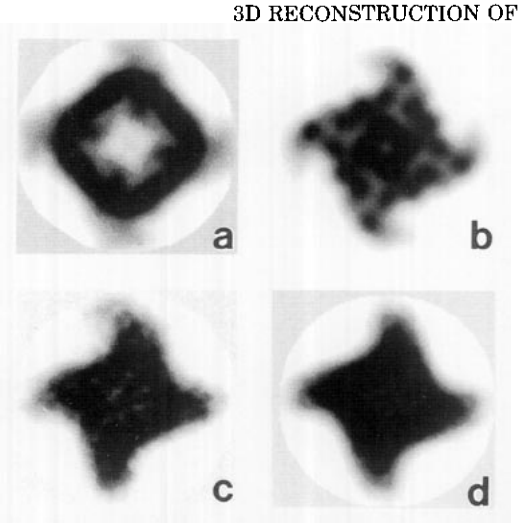

FIG. 5. Transverse (a and b) projections of the 3D density maps shown in Figs. 4c and 4d, respectively; (c) average and (d) rotationally filtered image calculated from transverse sections of freeze-substituted tarantula muscle (see Padrón *et al.,* 1993). In (a–d) the filaments were scaled radially to have the same diameter. To facilitate comparison with the positively stained (rapidly frozen) specimens, the contrast of the projections in (b) (negatively stained specimens) was reversed.

data on tarantula myosin filaments derived from other techniques. The Fourier transforms of the rapidly frozen filaments are similar to those of negatively stained and of frozen-hydrated filaments and to the myosin component of X-ray diffraction patterns of intact tarantula muscle. This suggests that the helical crossbridge arrangement has been fairly well preserved. An important difference seen in the transforms from rapidly frozen filaments when compared with other data is that the fourth layer line in particular, but also the third and higher layer lines, are weak (Fig. 2a). In contrast, X-ray diffraction of intact tarantula muscle (J. Wray, personal communication) and Fourier transforms of negatively stained, isolated tarantula filaments (Fig. 2b; cf. Crowther *et al.,* 1985) and of frozen-hydrated tarantula filaments (preliminary unpublished data in collaboration with P. Vibert) show stronger fourth and higher myosin layer lines. Computation of Fourier transforms of model structures that contain four helices of two heads arranged similarly to the array shown in Fig. 4b also shows the presence of a strong fourth and higher layer lines.

The weakness of the higher-order layer lines suggests that the myosin heads in rapidly frozen, freeze-substituted filaments become disordered in the direction corresponding to the weaker layer lines, or that the tannic acid used in the substitution or some other effect may have filled in the finer density features corresponding to these higher-order layer lines. The presence of a strong fourth and higher layer lines in Fourier transforms of frozen-hydrated tarantula filaments shows that these changes do not occur during the freezing, but in the subsequent freeze-substitution or embedding.

An independent test of the reconstructions comes from comparison with transversely cut sections of rapidly frozen muscle (Fig. 5; Padrón *et al.,* 1992). The similarity between such sections and transverse projections of the reconstructions from both negatively stained and rapidly frozen, freeze-substituted specimens provides support for the reconstructions (Figs. 5a, and 5b; cf. Figs. 5c and 5d) without the assumption of a helical structure.

While our reconstruction of filaments in the intact filament lattice supports that from negatively stained, isolated filaments, the resolution of the latter is higher. Examination of this earlier map led to the interpretation that the two heads of each myosin molecule were splayed apart, with one pointing along the long-pitch helix toward the bare zone and the other pointing in the opposite direction (Crowther *et al.,* 1985; cf. Stewart *et al.,* 1985). This antiparallel, overlapping arrangement of the heads (Fig. 4b) has been supported by crosslinking studies (Levine *et al.,* 1988; Levine, 1993) and suggests a simple mechanism by which regulatory light chain phosphorylation could modulate contraction (Crowther *et al.,* 1985; Craig *et al.,* 1987; Padrón *et al.,* 1991; see also Sweeney *et al.,* 1993), involving interaction between heads from axially adjacent myosin molecules. Approximate fitting of the atomic structure of S1 (Rayment *et al.,* 1993) to the reconstruction suggests that such interaction involves the 50-kDa domains of the heads, but that the light chain regions of different myosin molecules do not interact with each other (Fig. 4e). We are currently performing three-dimensional fitting of the S1 α-carbon atomic coordinates into the envelope of the reconstruction computationally, in order to define more precisely the location of the domains and active sites on the myosin head.

In conclusion, our observations have shown that it is possible to preserve major features of the relaxed structure of myosin filaments by rapid freezing followed by freeze-substitution in the presence of tannic acid. However, fine features are lost during the procedure, and improvements are required to minimize these alterations. Such changes come about even with myosin filaments, such as tarantula, have a stable relaxed crossbridge array. The possibility of such alterations should be taken into account when rapid freezing, freeze-substitution techniques are used to interpret fine details of crossbridge structure in more labile myosin filaments as well as in contracting muscle (Tsukita and Yano, 1985, 1986, 1988; Padrón *et al.,* 1988; Lepault *et al.,* 1991; Hirose and Wakabayashi, 1991, 1993; Hirose *et al.,* 1993; Sosa *et al.,* 1994).

We are especially grateful to Dr. Peter Vibert for advice concerning the 3D reconstructions, Dr. R. A. Crowther for providing the original Bessel-separated data published in Crowther *et al.* (1985), and Dr. Ivan Rayment for permission to use the space filling representation of S1. We thank Dr. Rodrigo Medina for help in debugging the Bessel separation program to run on SunOS UNIX and Pedro Medina, Mardonio Diaz, Omaira Gonzalez, Jorge Rivas, and Christine Dunshee for skillful photographic help. We would like to dedicate this paper to the memory of Dr. Carlos Schubert. This work was supported by grants from NIH (AR 34711 to R.C.), the Muscular Dystrophy Association (to R.C. and to R.P.), and CONICIT (S1-2006 to R.P.).

REFERENCES

Craig, R., Padrón, R., and Kendrick-Jones, J. (1987) Structural changes accompanying phosphorylation of tarantula muscle myosin filaments, *J. Cell Biol.* **105,** 1319–1327.

Craig, R., Padrón, R., and Alamo, L. (1991) Direct determination of myosin filament symmetry in scallop striated adductor muscle by rapid freezing and freeze-substitution, *J. Mol. Biol.* **220,** 125–132.

Craig, R., Alamo, L., and Padrón, R. (1992) Structure of the myosin filaments of relaxed and rigor vertebrate striated muscle studied by rapid freezing electron microscopy, *J. Mol. Biol.* **228,** 474–487.

Crowther, R. A., Padrón, R., and Craig, R. (1985) Arrangement of the heads of myosin in relaxed thick filaments from tarantula muscle, *J. Mol. Biol.* **184,** 429–439.

Edelman, L. (1989) The contracting muscle: A challenge for freeze-substitution and low temperature embedding, *Scanning Microsc. Suppl.* **3,** 241–252.

Heuser, J. E., and Cooke, R. (1983) Actin–myosin interactions visualized by the quick-freeze, deep-etch replica technique, J. Mol. Biol. **169,** 97–122.

Hirose, K., and Wakabayashi, T. (1988) Thin filaments of rabbit skeletal muscle are in helical register, *J. Mol. Biol.* **204,** 797–801.

Hirose, K., and Wakabayashi, T. (1991) Conformations of crossbridges in contracting skeletal muscle, *Adv. Biophys.* **27,** 197–203.

Hirose, K., and Wakabayashi, T. (1993) Structural change of crossbridges of rabbit skeletal muscle during isometric contraction, *J. Muscle Res. Cell Motil.* **14,** 432–445.

Hirose, K., Lenart, T. D., Murray, J. M., Franzini-Armstrong, C., and Goldman, Y. (1993) Flash and smash: Rapid freezing of muscle fibers activated by photolysis of caged ATP, *Biophys. J.* **65,** 397–408.

Huxley, H. E. (1963) Electron microscope studies on the structure of natural and synthetic protein filaments from striated muscle, *J. Mol. Biol.* **7,** 281–308.

Huxley, H. E. (1969) The mechanism of muscular contraction, *Science* **164,** 1356–1366.

Huxley, H. E., and Brown, W. (1967) The low angle x-ray diagram of vertebrate striated muscle and its behavior during contraction and rigor, *J. Mol. Biol.* **30,** 383–434.

Kensler, R. W., and Stewart, M. (1983) Frog striated muscle thick filaments are three-stranded, *J. Cell Biol.* **96,** 1797–1802.

Kensler, R. W., and Stewart, M. (1986) An ultrastructural study of cross-bridge arrangement in the frog thigh muscle thick filament, *Biophys. J.* **49,** 343–351.

Kensler, R. W., and Stewart, M. (1989) An ultrastructural study of crossbridge arrangement in the fish skeletal muscle thick filament, *J. Cell Sci.* **94,** 391–401.

Lepault, J., Erk, I., Nicolas, G., and Ranck, J. (1991) Time-resolved cryo-electron microscopy of vitrified muscular components, *J. Microsc.* **161,** 47–57.

Levine, R. J. C. (1993) Evidence for overlapping myosin heads on relaxed thick filaments of fish, frog, and scallop striated muscles, *J. Struct. Biol.* **110,** 99–110.

Levine, R. J. C., Kensler, R. W., Reedy, M. C., Hofmann, W., and King, H. A. (1983) Structure and paramyosin content of tarantula thick filaments, *J. Cell Biol.* **97,** 186–195.

Levine, R. J. C., Chantler, P. D., and Kensler, R. W. (1988) Arrangement of myosin heads on Limulus thick filaments, *J. Cell Biol.* **107,** 1739–1747.

McDowall, A. W., Hoffman, W., Lepault, J., Adrian, M., and Dubochet, J. (1984) Cryo-electron microscopy of vitrified insect flight muscle, *J. Mol. Biol.* **178,** 105–111.

Morris, E. P., Squire, J. M., and Fuller, G. W. (1991) The 4-stranded helical arrangement of myosin heads on insect (*Lethocerus*) flight muscle thick filaments, *J. Struct. Biol.* **107,** 237–249.

Nassar, R., Wallace, N. R., Taylor, I., and Sommer, J. R. (1986) The quick-freezing of single intact skeletal muscle fibers at known time intervals following electrical stimulation, *Scanning Electron Microsc.* **1986,** 309–328.

Padrón, R., and Craig, R. (1989) Disorder induced in non-overlap myosin crossbridges by loss of ATP, *Biophys. J.* **56,** 927–933.

Padrón, R., Alamo, L., Craig, R., and Caputo, C. (1988) A method for quick-freezing live muscles at known instants during contraction with simultaneous recording of mechanical tension, *J. Micros.* **151,** 81–102.

Padrón, R., Panté, N., Sosa, H., and Kendrick-Jones, J. (1991) X-ray diffraction study of the structural changes accompanying phosphorylation of tarantula muscle, *J. Muscle Res. Cell Motil.* **12,** 235–241.

Padrón, R., Granados, M., Alamo, L., Guerrero, J. R., and Craig, R. (1992) Visualization of myosin helices in sections of rapidly frozen relaxed tarantula muscle, *J. Struct. Biol.* **108,** 269–276.

Padrón, R., Guerrero, J. R., Alamo, L., Granados, M., Gherbesi, N., and Craig, R. (1993) Direct visualization of myosin filament symmetry in tarantula striated muscle by electron microscopy, *J. Struct. Biol.* **111,** 17–21.

Padrón, R., Alamo, L., Granados, M., Guerrero, J. R., Uman, P., Gherbesi, N., and Craig, R. (1994) Three-dimensional reconstruction of thick filaments from rapidly frozen, freeze-substituted tarantula muscle, *Biophys. J.* **66,** A74.

Rayment, I., Rypniewski, W., Schmidt-Base, K., Smith, R., Tomchick, D. R., Benning, M. M., Winkelman, D. A., Wesenberg, G., and Holden, H. M. (1993) Three-dimensional structure of myosin subfragment-1: A molecular motor, *Science* **261,** 50–58.

Reedy, M. K. (1976) Preservation of x-ray patterns from frog sartorius muscle prepared for electron microscopy, *Biophys. J.* **16,** 126a.

Reedy, M. K., Goody, R. S., Hoffman, W., and Rosenbaum, G. (1983) Co-ordinated electron microscopy and x-ray studies of glycerinated insect flight muscle. I. X-ray diffraction monitoring during preparation for electron microscopy of muscle fibres fixed in rigor, in ATP and AMPPNP, *J. Muscle Res. Cell Motil.* **4,** 25–53.

Sosa, H., Popp, D., Ouyang, G., and Huxley, H. E. (1994) Ultrastructure of skeletal muscle fibers studied by a plunge quick freezing method: myofilament lengths, *Biophys. J.* **67,** 283–292.

Squire, J. M. (1971) General model for the structure of all myosin-containing filaments, *Nature* **233,** 457–462.

Stewart, M., and Kensler, R. W. (1986) Arrangement of myosin

heads in relaxed thick filaments from frog skeletal muscle, *J. Mol. Biol.* **192,** 831–851.

Stewart M., Kensler, R. W., and Levine, R. J. C. (1981) Structure of Limulus telson muscle thick filaments, *J. Mol. Biol.* **153,** 781–790.

Stewart, M., Kensler, R. W., and Levine, R. J.C. (1985) Three-dimensional reconstruction of the thick filaments from Limulus and scorpion muscle, *J. Cell Biol.* **101,** 402–411.

Sweeney, H. L., Bowman, B. B., and Stull, J. T. (1993) Myosin light chain phosphorylation in vertebrate striated muscle: regulation and function, *Am. J. Phys. Cell Physiol.* **264,** C1085–C1095.

Tregear, R. T. (1984) The repeat distance of myosin in the thick filaments of various muscles, *J. Mol. Biol.* **176,** 417–420.

Tsukita, S., and Yano, M. (1985) Actomyosin structure in contracting muscle detected by rapid freezing, *Nature* **317,** 182–184.

Tsukita, S., and Yano, M. (1986) The ultrastructure of contracting skeletal muscle: a freeze-substitution and freeze-etch replica study, *in* Ishikawa, H., Hatano, S., and Sato, H. (Eds.), Cell Motility: Mechanism and Regulation, pp. 77–87, A. R. Liss, New York.

Tsukita, S., and Yano, M. (1988) Instantaneous view of actomyosin structure in shortening muscle, *in* Sugi, H., and Pollack, G. H. (Eds.), Molecular Mechanism of Muscle Contraction, pp. 31–38, Plenum, New York.

Vibert P. (1992) Helical reconstruction of frozen-hydrated scallop myosin filaments, *J. Mol. Biol.* **223,** 661–671.

Vibert, P., and Craig, R. (1983) Electron microscopy and image analysis of myosin filaments from scallop striated muscle, *J. Mol. Biol.* **165,** 303–320.

Wray, J. S. (1982) Organization of myosin in invertebrate thick filaments, *in* Twarog, B. M., Levine, R. J. C., and Dewey, M. M. (Eds.), Basic Biology of Muscles: A Comparative Approach, pp. 29–36, Raven Press, New York.

Wray, J. S., Vibert, P. J., and Cohen C. (1975) Diversity of cross-bridge configurations in invertebrate muscles, *Nature* **257,** 561–564.